

Multilevel Parametrization for Aerodynamical Optimization of 3D Shapes

Nathalie Marco and Alain Dervieux

N° 2949

Juillet 1996

———— THÈME 4 ————



***apport
de recherche***

Multilevel Parametrization for Aerodynamical Optimization of 3D Shapes

Nathalie Marco^{*} and Alain Dervieux^{*}

Thème 4 — Simulation et optimisation
de systèmes complexes
Projet Sinus

Rapport de recherche n° 2949 — Juillet 1996 — 27 pages

Abstract: We introduce and discuss a combination of methods and options that aim at the aerodynamical optimization of a flow around an arbitrary aircraft shape. The flow is governed by the Euler equations, discretized by a Mixed Element-Volume method on a fixed unstructured tetrahedrization. The shape parametrization relies on the skin of the above mesh through a hierarchical representation. Descent-type and One-Shot algorithms are devised and adapted to the solution of a few model problems.

Key-words: Computational fluid dynamics - Shape optimal design - Gradient method - Shape parametrization - Steepest descent - Optimization - Multilevel optimization - Euler equations - Unstructured mesh - Transpiration conditions

(Résumé : *tsvp*)

^{*} INRIA, 2004 Route des Lucioles, BP. 93, 06902 Sophia Antipolis Cédex-France

Paramétrisation multi-niveau pour l'optimisation de formes aérodynamiques 3D

Résumé : Nous proposons et discutons une combinaison de méthodes et d'options destinées à l'optimisation aérodynamique de la forme d'un avion plongé dans un écoulement d'air. L'écoulement est modélisé par les équations d'Euler, discrétisées par une méthode mixte élément/volume sur une tétraédrisation non structurée. La paramétrisation de la forme s'appuie sur le maillage de peau par l'intermédiaire d'une représentation hiérarchique. Des algorithmes de type descente et "one-shot" sont adaptés à la solution de quelques problèmes modèles.

Mots-clé : mécanique des fluides numérique - optimisation de forme - méthode de gradient - Paramétrisation de forme - plus grande descente - optimisation - optimisation multi-niveau- équations d'Euler - maillage non-structuré - conditions de transpiration

Contents

1	Scope of the paper	4
2	The importance of a continuous metrics	5
2.1	Continuous and discrete metrics	5
2.2	Unstructured multilevel optimization	7
3	From Hadamard to the gradient method	10
3.1	Parametrization and differentiability	10
3.2	Formal derivation of the gradient for Euler	12
3.3	Which pivot space for a Gradient method ?	13
4	Multilevel algorithms for shape optimization	13
4.1	Multilevel parametrization for 3D shapes	13
4.2	The multilevel algorithms : Gradient, One-Shot	14
5	Application to 3D aerodynamics	15
5.1	Global approach	15
5.2	A few examples	17
6	Conclusion	25
	References	27

1 Scope of the paper

Optimal shape design in aerodynamics is getting maturity and will reach in the next five years the point where best analysis codes (Navier-Stokes) will be involved in a loop optimizing thousands shape parameters.

Since both parameters and flow variables will be represented by a large number of unknowns, it becomes important to derive efficient solution/optimization methods with a moderate complexity when the number of variables is increased.

We observe that the complexity question is addressed for flow solution by many works, with some success when Multi-Grid (MG) algorithms are used ; these algorithms display a convergence rate that does not degrade when the number of unknowns is increased. We concentrate in this paper on the optimization problem and we look for algorithms that would also have a convergence rate insensitive to the number of optimized parameters.

One first essential option is to choose the way to parametrize the shape. Due to the necessity to face many numerical difficulties (slow convergence, oscillations), numerous authors have preferred the introduction of CAD-type parametrizations (splines, ...). This allows smooth shapes and fast convergence mainly because the number of effective parameters is small. Conversely, when the number of these spline parameters is significantly larger, oscillations appear.

Now, the large number of parameters is sometimes felt as a necessity to find shapes satisfying the whole set of constraints.

In this paper, we connect parametrization with solution algorithm and show that some functional analysis may help to build a regular multilevel parametrization.

One second essential option is to compute sensitivity, that is derivative of important quantities (at least the functional to minimize) with respect to parameters ; in fact, most minimization processes rely on sensitivity ; but when the variations are computed by divided differences, the computational cost usually exceeds n times the cost of one functional evaluation where n is the number of parameters.

Contrarily, solving an adjoint system for computing the gradient of the functional is no more costly than computing only one functional and yields n informations. This point of view is not very new (see for example [10]), but generates certain practical problems when writing the differentiated code ; one answer is automated or assisted differentiation ([2],[20]).

With differentiation (automated or by hand), large 3D geometries in Eulerian flow could be handled in a gradient loop ; one typical example is given by [19]. A. Jameson's optimization method presents a good convergence for rather heavy meshes and for a large number of control parameters ; we discuss this strategy in the sequel.

A second path to less costly optimization allowed by the derivation of an adjoint system is to solve simultaneously the combination of state system (the flow), adjoint system, and optimality equation related to the gradient of functional. This is suggested by Ta'asan et al. as a “one-shot” method [8].

Once the problem is formulated as a minimization problem with gradient, or as an optimality system, it is possible to combine the iterative search for the unknowns with a multi-grid or a multilevel method. In the sequel we call multi-grid a method in which a less complex system is built, based on coarser grid approximation ; in contrast, in the multilevel method that we propose, corrections are always computed from the unique fine grid, and multilevelling is operated through preconditioning.

Our contribution is to build a multilevel method relying on a gradient approach, applicable to the **unstructured** representation of a shape as the skin of a 3D tetrahe-
drization. For this purpose, we apply the volume-agglomeration principle introduced in [9] for unstructured multi-grid solution of Euler flows.

The relation between levels is revisited ; new transfer operators are derived for a cheap coarse-level projection. Properties of the proposed method are analysed in a simplified context (following [4]) for which the main features of the method are recalled.

The multilevel method is introduced either in an optimization loop or in a one-shot iteration. Its interest is demonstrated by an application to 3D aerodynamical shape optimization in which the shape variation is accounted for by a transpiration boundary condition, as recommended by D. Young and co-workers in [7], and which ensures that the functional is rigorously a differentiable one.

The paper is organized as follows : in a first section, we discuss the interest of choosing a functional or continuous metrics for optimization ; the multilevel optimization algorithm is introduced for a simplified model problem. In a second section we overview the main questions arising in the derivation of the gradient of the solution of a Partial Differential Equation. In the third section, we introduce the multilevel agglomeration method for shape optimization. In the last section, we present some applications to 3D aerodynamics.

2 The importance of a continuous metrics

2.1 Continuous and discrete metrics

Let us write a second-order elliptic continuous (= not discretized) Partial Differential Equation as follows :

$$A u = f \text{ on } \Omega \quad (1)$$

and its discretization :

$$A_h u_h = f_h \text{ on } \Omega. \quad (2)$$

A natural idea for solving (2) is to put :

$$u_h^{n+1} = u_h^n - \rho(A_h u_h - f_h) ; \quad (3)$$

An alarming remark for (3) is that it has no reasonable continuous counterpart since

$$u^{n+1} = u^n - \rho(A u - f) \quad (4)$$

would not produce a smooth enough u^{n+1} for computing Au^{n+1} in the next iteration. We note in passing that this kind of accident has motivated the development of smoothing operators used in the Nash-Moser theorem (see [16]) ; another way to build a *continuous iteration* is to introduce a *pivot metrics*, defined by a Sobolev space H^1 and its scalar product :

$$< u, v >_{H^1} = \beta \int_{\Omega} \nabla u \cdot \nabla v \, d\Omega + \int_{\Omega} uv \, d\Omega ; \quad (5)$$

Here, the real positive parameter β is introduced for showing that many metrics are possible for H^1 , and we shall put in the sequel $\beta = 1$.

For simplicity, we assume that (1) involves Dirichlet boundary conditions on $\partial\Omega$ so that, introducing the subspace H_0^1 of functions of H^1 that vanish on the boundary of Ω , we have :

$$A : H_0^1 \longrightarrow (H_0^1)' \quad (6)$$

where $(H_0^1)'$ is the topological dual of H_0^1 . Now, there exists a canonic isomorphism :

$$\Lambda : (H_0^1)' \longrightarrow H_0^1 \quad (7)$$

defined as follows :

$$(g, u)_{(H_0^1)' \times H_0^1} = < \Lambda g, u >_{H^1} \quad (8)$$

and explicitly computed by solving the *Poisson equation* :

$$\Delta \Lambda g = g \text{ on } \Omega, \quad \Lambda g = 0 \text{ on } \partial\Omega. \quad (9)$$

Then, we can consider the *continuous* algorithm :

$$u^{n+1} = u^n - \rho \Lambda(A u - f). \quad (10)$$

In the case where A is symmetric, (10) is a Functional Least Square algorithm *à la* Glowinski *et al.* [3] for minimizing by a gradient iteration the functional whose gradient is $Au - f$.

The interest in building an algorithm for the continuous model is that the continuous algorithm has a convergence rate that cannot be influenced by the mesh size. Then we can try to build some consistent discretization that will hopefully converge at a rate not so different from the continuous rate. This means that *essentially mesh*

independent rates are anticipated.

Conversely, for a typical discrete iteration such as (3), it is well known that this Jacobi-like iteration has a strongly mesh-dependent convergence rate.

More generally, the minimization of a functional j :

$$j : H_0^1 \longrightarrow \mathbb{R} \quad (11)$$

can be done by a gradient iteration relying on the functional operator Λ :

$$u^{n+1} = u^n - \rho \Lambda j'(u^n). \quad (12)$$

We recall that applying (12) while replacing Λ by the identity is possible only in discretized versions (by identifying two Euclidean spaces) :

$$u_h^{n+1} = u_h^n - \rho j_h'(u_h^n). \quad (13)$$

conversely, in the continuous case, Λ , has to be a mapping from $(H_0^1)'$ onto H_0^1 as defined in (7), (8) for giving a meaning to (12).

Again we claim that discretized versions of (12) will have better chances to converge at a rate independent of mesh size than (13). The latter option is still used frequently, while the former was chosen for example by A. Jameson [19] and B. Mohammadi in [14].

An alternative option is to solve the problem by a multilevel method using an adequate functional norm.

2.2 Unstructured multilevel optimization

We turn now to the main focus of this paper, *the application of a multilevel optimization algorithm*. Again the identification of an adequate continuous metrics is of paramount importance. This point is analysed in details in [4] for the minimization of the above quadratical functional (the Poisson problem) in the case of unstructured meshes. We summarize now the main results of that study.

We consider the minimization problem :

$$\text{Find } \bar{u} \in V \text{ such that } \bar{u} = \underset{u \in V}{\text{Arg min}} j(u) \quad (14)$$

where V is a Hilbert space (think of a Sobolev space) and where the cost functional j is continuous for the functional norm of V and corresponds to the 2D Poisson equation :

$$j(u) = \int \int_{\Omega} \left(\frac{1}{2} \|\nabla u\|^2 - fu \right) dx dy. \quad (15)$$

We investigate the application of the multilevel optimization to Problem (14) in order to put in evidence the basic options that will allow an efficient multilevel solution.

The multilevel optimization method needs several coarse levels. For this purpose, from any triangulation \mathcal{T}_h , we introduce a dual finite volume partition built with median cells. In Figure 1, a cell (or volume control) is presented. It is obtained by connecting the midpoints of sides adjacent to node i with the centroids of the triangles such that i is a vertex.

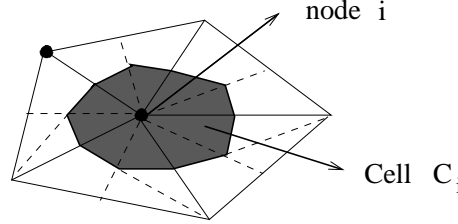


Figure 1: Cell control.

Then, a coarser finite volume is obtained by grouping or agglomerating the above cells. For this purpose, a coarsening algorithm (see [9] for more details) is defined in the following process :

Each cell i is considered successively :

- (i) *if the current cell i has already been included in a coarse zone then **goto** (ii) ;
else create a new zone I containing the cell i , and neighboring cells j which do not already belong to another previously defined coarse zone ;*
- (ii) *if all the cells have been colored **stop**, else consider the next cell i and **goto** (i).*

In Figure 2, we give an example of the construction of coarse meshes from a fine mesh of a 2D profile of a NACA0012 airfoil.

Let us write a *coarse level correction* as follows :

$$u_{2h}^{n+1} = u_{2h}^n - \rho_{opt} \mathcal{L} \mathcal{P} \mathcal{P}^* \mathcal{L}^* j'(u_{2h}^n). \quad (16)$$

In (16), \mathcal{P} is a canonical prolongation operator from coarse level to fine level :

$$\forall u_{2h} \in V_{2h} \quad \mathcal{P} u_{2h} = u_{2h} \in V_h \quad (17)$$

where $V_h = [\varphi_i, i = 1 \cdots n_h / P1 \text{ Galerkin basis functions}]$ is the discrete fine space and $V_{2h} = [\Phi_J, J = 1 \cdots n_{2h} / \Phi_J = \sum_{i \in I_J} \varphi_i]$ (I_J , for a given J , is a subset of the fine indices set) is the discrete coarse space. \mathcal{P}^* , the transpose of \mathcal{P} , is a restriction operator from fine level to coarse level. \mathcal{L} is an average smoothing operator (\mathcal{L}^* is its

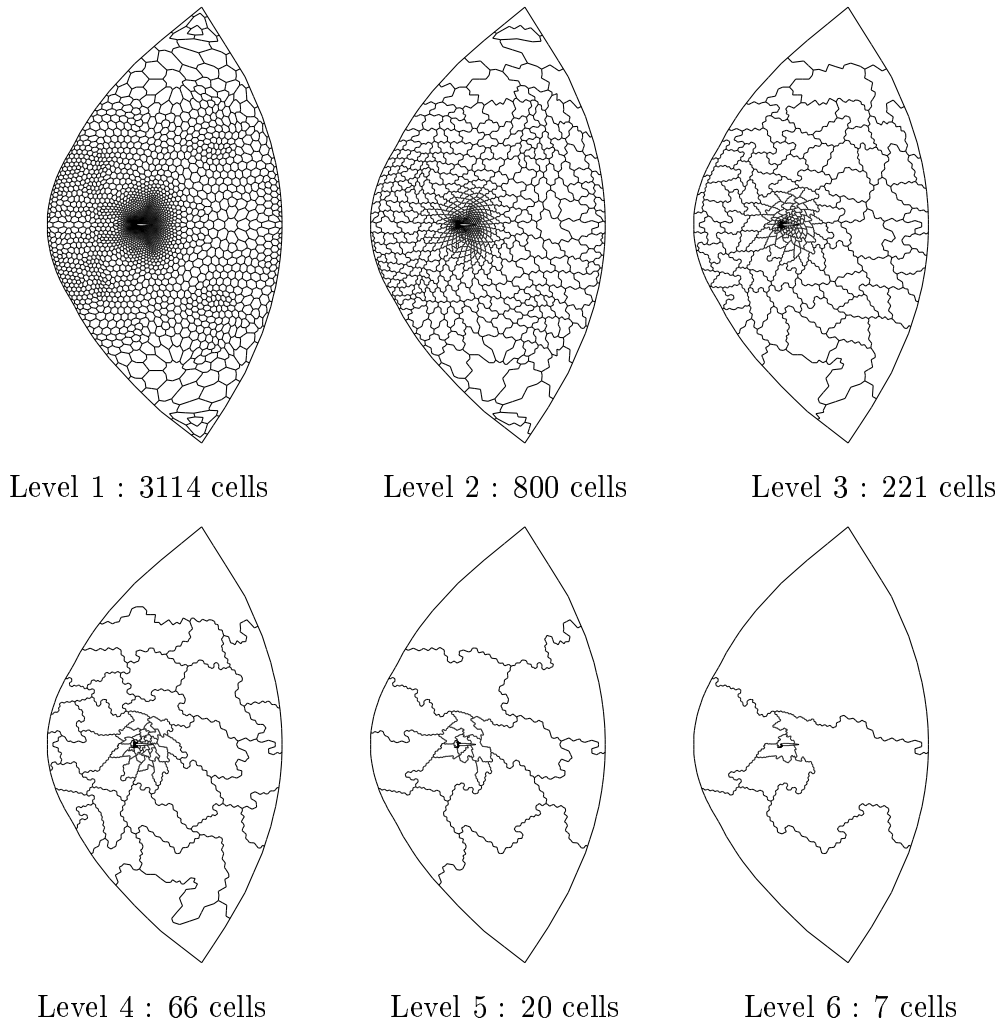


Figure 2: The successive levels of an initial fine mesh of 3114 nodes.

transpose) defined by :

$$(\mathcal{L}u_h)_i = (1 - \theta)(u_h)_i + \theta \frac{\sum_{j \in \mathcal{N}(i) \cup \{i\}} \text{Area}(j) (u_h)_j}{\sum_{j \in \mathcal{N}(i) \cup \{i\}} \text{Area}(j)} \quad (18)$$

in which Area is the measure of the finite-volumes cells built around vertices with medians.

A key condition for efficiency is that the fixed point u_{2h}^* of (16) which satisfies $\mathcal{LPP}^* \mathcal{L}^* j'(u_{2h}^*) = 0$, be a *convergent approximation* of $\text{Argmin } j$ when the mesh size is increased ; in other words :

$$u_{2h}^* \xrightarrow{h \rightarrow 0} \bar{u} \quad (19)$$

A necessary condition for (19) is that the transfer operator $\mathcal{P}^*\mathcal{L}^*$ is V-regular, according to the following definition :

Définition 2.1 $\mathcal{P}^*\mathcal{L}^*$ is V-regular if $\forall v \in V, \forall \varepsilon > 0, \exists v_h \in V_h$ such that $\|\mathcal{P}^*\mathcal{L}^*v_h - v\|_V < \varepsilon$.

It is shown in [4] and [11] that under certain conditions, the transfer $\mathcal{L}\mathcal{P}$ and its transpose $(\mathcal{P}^*\mathcal{L}^*)$ are H^1 regular. Then, similarly to the standard multigrid theory (see [5]), in which the so-called “approximation property” ensures the adequacy of the coarse grid corrections, Property (19) allows to derive a V-cycle strategy, relying on (16) applied to different levels, for which convergence speed is mesh-size independent. This is sketched on Figure 3 for the multilevel method (16) for the solution of the Poisson equation on several unstructured meshes.

In this academic example, the pivot space is clearly $V = H^1(\Omega)$ and we have built a multilevel method that is regular for these metrics.

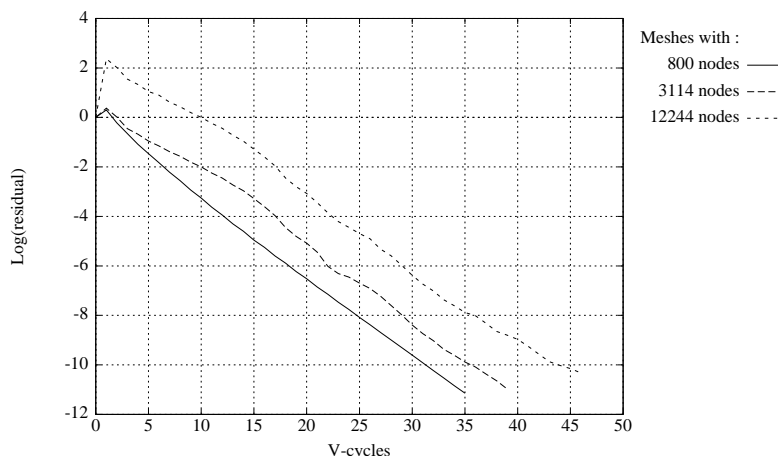


Figure 3: Multilevel optimization for solving the Poisson equation (convergence history of the gradient for several unstructured fine levels ; for each case at least five agglomerated coarse levels).

3 From Hadamard to the gradient method

The functional considered in a shape optimization problem is not quadratic. The purpose of the present section is to overview the available information hidden in the continuous shape-optimization functional for better understanding the discrete context.

3.1 Parametrization and differentiability

We start from some known differentiability results applicable to *shape perturbation of the Poisson problem* ; these results can be found in many publications such as [17].

We emphasize that the above theory is today not *rigorously* applicable to the compressible Euler or Navier-Stokes systems. When we shall need a complete theory for discussion, we shall refer to the Poisson problem ; when we shall try to derive heuristically analogous remarks for the Euler system, we shall use some *formal* derivation.

We parametrize a set of simply connected (for simplicity) geometrical domains by introducing the following notations :

Let Ω_0 be a simply connected fixed open subset of \mathbb{R}^2 with a smooth boundary. Its boundary curvilinear abscissa varies from 0 to 2π .

Let Γ_{ad} be a set of parameters included in $C^1([0, 2\pi], \mathbb{R}^2)$, that we assume to be (strictly) positive ; for any function γ of Γ_{ad} , we define Ω_γ as the regular domain of \mathbb{R}^2 , whose boundary is obtained by moving boundary points of Ω_0 along its normal vector \vec{n}_0 for an algebraic length of γ .

$$\partial\Omega_\gamma = \{ \vec{x} + \gamma(\vec{x})\vec{n}_0(x) ; x \in \partial\Omega_0 \}$$

Let us consider the following functional :

$$\forall \gamma \in \Gamma_{ad}, \quad j(\gamma) = \frac{1}{2} \|z(\gamma) - z_{target}\|_{L^2(\Omega_0)}^2,$$

where $z_{target} \in L^2(\Omega_0)$ is given and where $z(\gamma)$ is a solution of (20) :

$$-\Delta z(\gamma) = 1 \text{ in } \Omega_\gamma ; \quad z(\gamma) = 0 \text{ on } \partial\Omega_\gamma. \quad (20)$$

In [17] it is shown that the functional j is **differentiable** with respect to γ when γ varies in $W^{1,\infty}(0, 2\pi)$, further, when functions are smooth enough, its gradient is given by :

$$j'(\gamma).\delta\gamma = \int \left(\frac{\partial z(\gamma)}{\partial n} \right) \left(\frac{\partial p(\gamma)}{\partial n} \right) < \vec{n}_0, \vec{n}_\gamma > \delta\gamma \, d\sigma \quad (21)$$

where the integral is taken on $\partial\Omega_\gamma$, \vec{n}_γ is the normal vector on $\partial\Omega_\gamma$, and where $p(\gamma)$ is the adjoint state, solution of the adjoint equation :

$$-\Delta p(\gamma) = 2\chi_{\Omega_0}(z(\gamma) - z_{target}) \text{ in } \Omega_\gamma ; \quad z(\gamma) = 0 \text{ on } \partial\Omega_\gamma. \quad (22)$$

Whether the chosen norm, $W^{1,\infty}$, is optimal or not, is an open question ; clearly, if the state variable $z(\gamma)$ is smooth enough, then the Gateaux-derivative depicted in (21) is well defined for any $\delta\gamma$ belonging only in $L^2(0, 2\pi)$, but this does not mean at all that differentiability holds in this space ! In particular, expression (21) involves the first derivative of γ through its normal \vec{n}_γ , which indicates that (at least) a H^1 -regularity of γ may be necessary for continuous differentiability.

3.2 Formal derivation of the gradient for Euler

In [1], a formal computation is proposed for the Hadamard formula related to the steady Euler system for compressible gas. We recall it now.

The state system is the following one :

$W(\gamma)$ is a solution of (23) :

Find $W = (W_1, W_2, W_3, W_4) = (\rho, \rho u, \rho v, E)$ such that for all $\varphi = (\varphi_1, \varphi_2, \varphi_3, \varphi_4)$,

$$- \int \int_{\Omega_\gamma} (F(W) \varphi_x + G(W) \varphi_y) dx dy + \int_\gamma \begin{pmatrix} 0 \\ P(W)n_x^\gamma \\ P(W)n_y^\gamma \\ 0 \end{pmatrix} \varphi d\sigma = 0. \quad (23)$$

$\vec{n}_\gamma = (n_x^\gamma, n_y^\gamma)$ is the unitary outward normal vector on γ , P the boundary pressure and F and G the eulerian flux functions.

The cost functional is now written :

$$\forall \gamma \in \Gamma_{ad}, \quad j(\gamma) = \frac{1}{2} \|P(W(\gamma)) - P_{target}\|_{L^2(\Omega_0)}^2,$$

where $P(W(\gamma))$ is the pressure corresponding to the flow field $W(\gamma)$ (i.e. according to state law) and P_{target} a target pressure.

Since $j(\gamma)$ is real-valued, the chain-rule for its differentiation is again applied by introducing an adjoint-system :

$$\left\{ \begin{array}{l} \pi(\gamma) = (\pi_1, \pi_2, \pi_3, \pi_4) \\ \left(\frac{\partial F}{\partial W} \right)^* \pi_x + \left(\frac{\partial G}{\partial W} \right)^* \pi_y = - \chi_{\Omega_0} \frac{\partial P}{\partial W} (P(W(\gamma)) - P_{target}) \quad \text{in } \Omega_\gamma \\ \left(\begin{pmatrix} \pi_2 \\ \pi_3 \end{pmatrix} \right) \cdot \vec{n}_\gamma = 0 \quad \text{on } \partial\Omega_\gamma \end{array} \right.$$

where χ_{Ω_0} is the characteristic function of Ω_0 .

Then, we have formally the Gateaux-derivative :

$$\begin{aligned}
 j'(\gamma, \delta\gamma) = & - \int_{\partial\Omega_\gamma} (F(W) \pi_x + G(W) \pi_y) \langle \vec{n}_0, \vec{n}_\gamma \rangle \delta\gamma \, d\sigma \\
 & + \int_{\partial\Omega_\gamma} \left(\begin{pmatrix} 0 \\ \frac{\partial P}{\partial x} \\ \frac{\partial P}{\partial y} \\ 0 \end{pmatrix} \pi + P \begin{pmatrix} 0 \\ \frac{\partial \pi_2}{\partial x} \\ \frac{\partial \pi_3}{\partial y} \\ 0 \end{pmatrix} \right) \langle \vec{n}_0, \vec{n}_\gamma \rangle \delta\gamma \, d\sigma.
 \end{aligned} \tag{24}$$

We observe again that, similarly to the Poisson case, this expression is well-defined as far as W is regular enough, $\delta\gamma$ and derivatives of γ are square integrable.

3.3 Which pivot space for a Gradient method ?

According to Section 1, we have to introduce a **Hilbert** space Γ , containing Γ_{ad} , for building a gradient method, written :

$$\gamma^* = \gamma - \rho \Lambda_\Gamma j'(\gamma);$$

since the gradient j' of j lies in the dual of the space of control Γ , it is necessary to apply an isomorphism Λ_Γ , mapping the dual Γ' of Γ into Γ , and related to the scalar product in Γ :

$$j'(\gamma) \cdot \delta\gamma = \langle \Lambda_\Gamma j'(\gamma), \delta\gamma \rangle_\Gamma \tag{25}$$

We consider now both space norms and gradient form. For rigor, we consider the case of the Poisson problem as state equation ; we have recalled in Section 3.1 that **differentiability** is true for boundaries varying in $W^{1,\infty}$ or C^1 .

Since a gradient method is to be built in a Hilbert space, we need a Hilbert space included in $W^{1,\infty}$; a direct application of the Sobolev inclusion theorem [18] allows to consider for 2D parameters a H^3 space (H^2 for 1D parameters). The choice of such a regular space is sufficient but we do not know whether it is necessary. For H^3 , this means that for obtaining the descent direction $\Lambda_\Gamma j'$ from (25), we would have to solve a 6-th order elliptic system !

Conversely, from (24), L^2 is necessary for Gateaux derivability, H^1 for continuous differentiability. In the sequel, we shall choose to work in H^1 .

4 Multilevel algorithms for shape optimization

4.1 Multilevel parametrization for 3D shapes

We now consider the parametrization for optimizing an aircraft in a 3D Euler flow ; the parametrized shape is then a 3D surface and flow calculations are performed on an

unstructured 3D mesh. The construction of a multilevel parametrization ([1]) of this shape will rely on a node-agglomeration principle (see [13]).

The surface is assimilated to a smooth enough manifold Σ . The discrete geometry Σ_h is the surfacic boundary of a 3D unstructured tetrahedrization and is made of triangles in 3D. A deformation provoked on Σ_h , is noted $\delta\Sigma_h$; the new manifold $\Sigma_h + \mathcal{L}\mathcal{P}\mathcal{P}^*\mathcal{L}^*\delta\Sigma_h$ is built by a projection \mathcal{P}^* to a coarser level, a prolongation \mathcal{P} , transpose of \mathcal{P}^* , to the initial level, combined with an operator \mathcal{L} (details are given in [13]). The smoothing operator \mathcal{L} is an average weighted by a scalar product of normals :

$$(\mathcal{L} \vec{x})_i = (1 - \theta)\vec{x}_i + \theta \frac{\sum_{j \in \mathcal{N}(i) \cup \{i\}} w_{ij} \vec{x}_j}{\sum_{j \in \mathcal{N}(i) \cup \{i\}} w_{ij}} \quad (26)$$

where w_{ij} are the weights defined by :

$$w_{ij} = \text{Max} (\text{Area}(i) \cdot \text{Area}(j) \cdot \vec{n}_i \cdot \vec{n}_j, 0) \quad \|\vec{n}_i\| = 1 \quad \forall i \quad (27)$$

and where $\mathcal{N}(i)$ represents neighbors of cell i and θ is the smoothing parameter.

This construction extends (17) (18) to a non flat manifold. In Figure 5, perturbation on level 3 is depicted for an aircraft shape ; the initial shape is given on Figure 4.

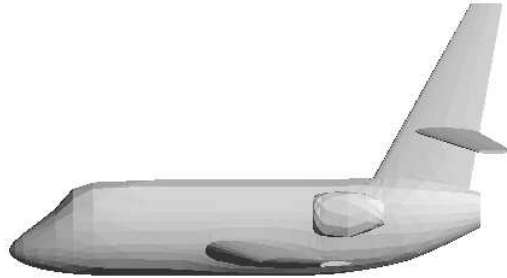


Figure 4: Initial shape of the aircraft.

4.2 The multilevel algorithms : Gradient, One-Shot

The multilevel gradient approach considered here is introduced in [1] ; it relies on the following algorithm (called *Multilevel algorithm*) :

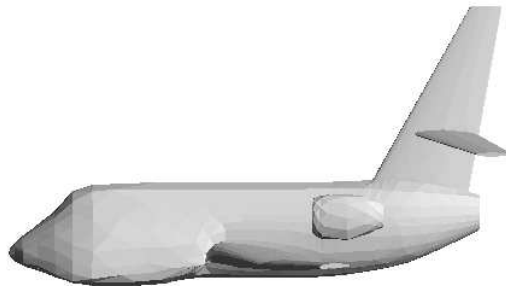


Figure 5: Perturbation on the 3rd level and smoothing.

For each cycle nc ,

For each level nl , $1 \leq nl \leq nlmax$,

Compute state and adjoint, compute G

$$\gamma^{nl+(nlmax-1)nc} = \gamma^{nl+(nlmax-1)nc-1} - \rho \mathcal{L}_{nl} \mathcal{P}_{nl} \mathcal{P}_{nl}^* \mathcal{L}_{nl}^* G$$

next nl

next nc .

where \mathcal{L}_{nl} and \mathcal{P}_{nl} are defined in Section 3.1, according to level nl , and where G is a function of two variables W and Π , that is identical to $j'(\gamma)$ only if $W = W(\gamma)$ (state equation) and $\Pi = \Pi(\gamma)$ (adjoint state equation). The parameter ρ is either fixed or defined by a 1D search.

This algorithm results in a kind of steepest-descent algorithm when G is exactly $j'(\gamma)$ and we refer to it as a **multilevel gradient method** [11] ; conversely, when W and Π are obtained by applying only a few iterations of an iterative solution algorithm to state and adjoint-state equations, then G is not the gradient of j , but aims to converge towards $j'(\gamma)$ when the whole loop is converging ; we refer to this algorithm as a **one-shot method** (according to [8]) for solving the optimality system of the optimization problem. The performance of this approach for 2D applications is discussed in [12].

5 Application to 3D aerodynamics

5.1 Global approach

The numerical method applied for predicting steady Euler flows, is a mixed element volume approximation involving the well-known Van Leer flux vector splitting. The overall differentiability of the process will allow to apply an exact-gradient approach.

The application of a shape design loop should involve the repeated rezoning of the mesh to account for the modification of the shape of the aircraft.

In this work, inspired by the approach used by Young *et al.* ([7]), we are considering in a first phase the option of representing the shape modification by applying a transpiration condition ; this means that the current shape is defined with respect to the mesh skin as a perturbation simulated by transpiration (see for example [15]), referred in the sequel as the “*transpired perturbation*”. Let us denote by γ the perturbation function ; it is the algebraic length of the displacement of the boundary along its normal.

We recall the transpiration condition for Euler flows :

Let us denote by *shell* the shape to be emulated by transpiration and by \vec{n}_{shell} the normal of the shell. The slip boundary term of the flux $\Psi(W)$ is defined as follows :

$$\Psi(W)_{slip\ boundary} = q\ W + \begin{pmatrix} 0 \\ p(W)\ n_x \\ p(W)\ n_y \\ p(W)\ n_z \\ p(W)\ q \end{pmatrix}$$

with :

$$q = \vec{V} \cdot (\vec{n} - \vec{n}_{shell})$$

where \vec{V} is the velocity of the fluid. This approximation has proved accurate enough for rather large perturbations of the boundary and very robust.

The sensitivity analysis has been derived exactly, but only for the first-order accurate upwind scheme. The linearization (by differentiation) of the transpiration condition is straightforward and an adjoint state is easily computed. The validation of this sensitivity is performed by a direct comparison with divided differences of the cost function ; errors in gradient components are of the order of 0.001 %.

The global method is essentially made of three loops (Figure 6). The external loop is a remeshing loop in which a new shape is derived from an old one updated by the transpired perturbation ; we still do not use it here. The medium loop is a gradient optimization loop in which the control variable is the transpired perturbation ; this loop involves the evaluation of the gradient of the cost functional through an adjoint state.

We have, in the previous sections, discussed in details the ability of the multilevel to converge with a speed that is rather insensitive to the number of parameters ; we now stress that, although easily obtained by the multilevel method, the optimal control can show spurious high frequencies. We think that the origin of an odd-even decoupling lies in the fact that normal vectors at nodes are (arithmetic) means of normal vectors to faces of the shape. From this point of view, the Euler flow is rather insensitive to high frequency oscillations of the boundary. This defect is amplified by the transpiration formulation in which high frequencies affect normals but not cell volumes ! Our answer to this problem is to avoid to use the finest level (which involves the whole set of

boundary node coordinates).

The most internal loop is the 1D local research of the steepest descent parameter ρ_{opt} .

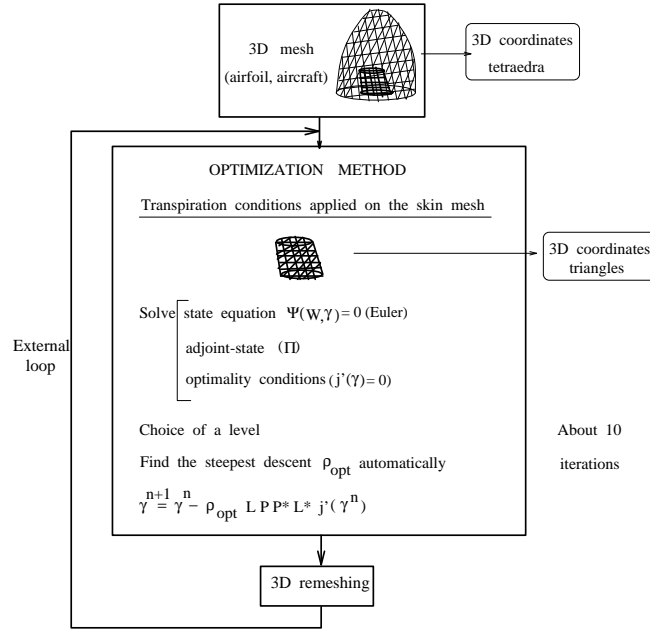


Figure 6: Organization of the optimization loop.

5.2 A few examples

The following examples rely on several very simplified problems. In proposing them, we aim to show how the application of the method to a new geometry is easy. Improving the efficiency of the flow solver has not been considered except by some tuning of Courant numbers and number of linear sweeps during the implicit time stepping.

5.2.1 Minimization of the shock drag on ONERA M6 wing using 15460 nodes.

The skin mesh of the wing is composed by 3819 nodes.

The cost functional we have used is of the form :

$$j(\gamma) = \omega_1 (C_D - C_D^{target})^2 + \omega_2 (C_L - C_L^{target})^2 + \omega_3 \int_{\gamma} (P - P^{target})^2 d\sigma$$

with $\omega_1 = 10$, $\omega_2 = 1$, $\omega_3 = 1$ and $C_D^{target} = 0$.

The initial conditions are defined by a farfield Mach number of 0.84 and an angle of attack of 3.06 degrees, which gives :

$$C_D^0 = 1.761e - 02 \quad \text{and} \quad C_L^0 = C_L^{target} = 0.145$$

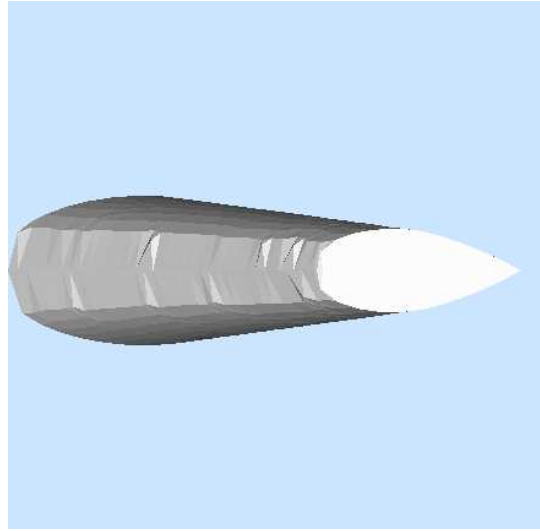


Figure 7: M6-wing optimization ; initial shape.

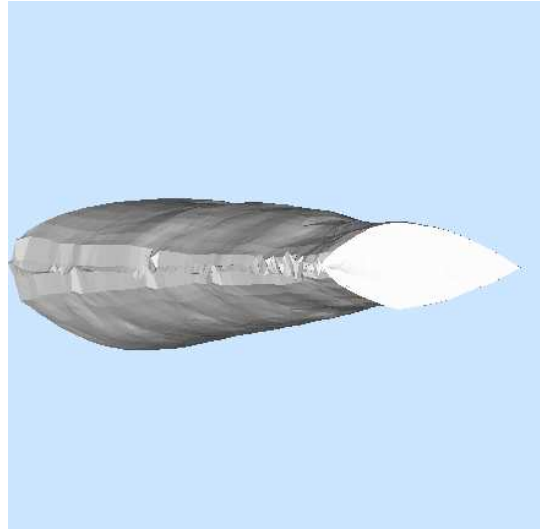


Figure 8: M6-wing optimization ; final shape after 10 optimization iterations.

We have used a sawtooth V-cycles strategy between the fourth level, with 59 parameters and the finest level. After 10 optimization iterations, the obtained drag is

$$C_D^{10} = 0.57 C_D^0 \quad \text{and} \quad C_L^{10} = 0.98 C_L^{target}$$

The CPU time is about 5 hours on a DEC station.

Figures 7 and 8 present the initial shape and the final shape. On Figure 9, we see a reduction of the shock on the wing.

5.2.2 Optimization of an aircraft (Falcon) with 10188 nodes.

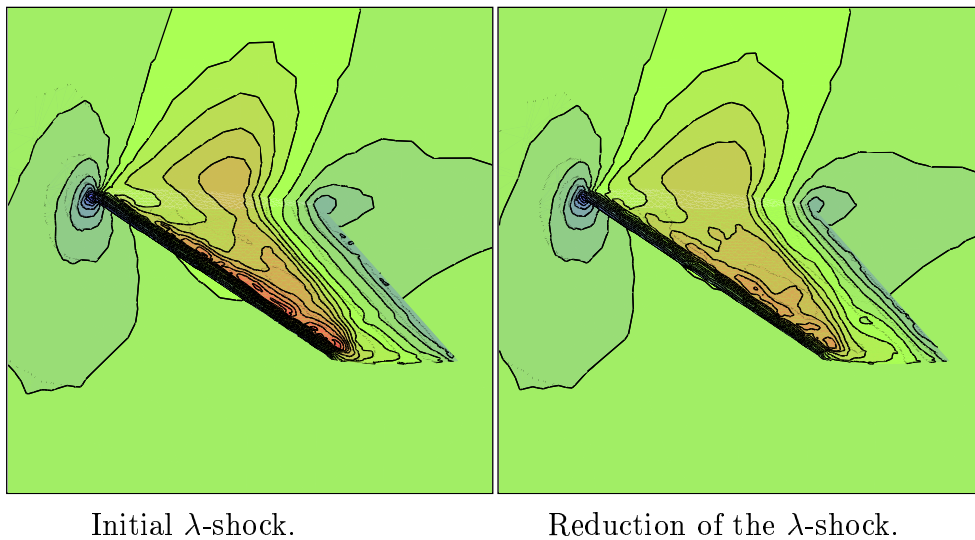


Figure 9: Reduction of the initial λ -shock after 10 optimization iterations.

The skin mesh of the aircraft is composed of 981 nodes.

The cost functional to be minimized is the same as the one for the M6 wing. The initial conditions are defined by a farfield Mach number of 0.85, with no incidence.

In our model study, we first consider a rather simple aerodynamical objective function that measures the smoothness of the pressure distribution on the aircraft fuselage. A first flow computation is made ; then the pressure distribution is regularized, and the regularized distribution is taken as a target one.

It is interesting to note that the sensitivity analysis can be seen by the user, as a rough estimation of the level of desirable displacement normally the wall ; it is positive when the aircraft skin should be threaded out, negative when it should be forced in (see Figure 10). We already observe that a constant body section is not optimal ; for example, the body should be narrower at the wing-junction stage (as intuitively indicated by the standard “area law”).

Our purpose is now to illustrate the ability of this kind of method in helping to optimize a shape by accounting for the interaction of the different part of the geometry. Optimizing the whole shape of such a complex geometry would demand the introduction of a lot of constraints. We shall prefer local improvements, but with a global analysis. We choose to concentrate on an effect related to higher pressures, near the pylon-body junction, and one related to lower pressures, after the cabin.

a- Reduction of the pressure peak in the body-pylon junction.

The influence of the body-pylon junction on pressure fluctuations is large. We choose to concentrate the optimization on the body shape near this junction. In Figure 9 are

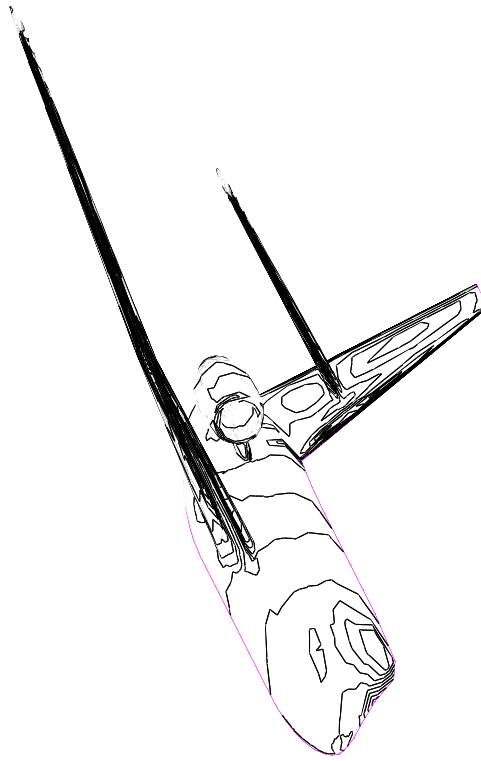
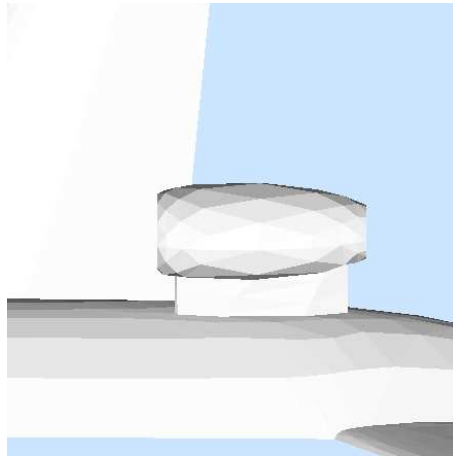


Figure 10: Research by shape optimization of a more uniform pressure on a Falcon aircraft : iso-gradients contours on the body.

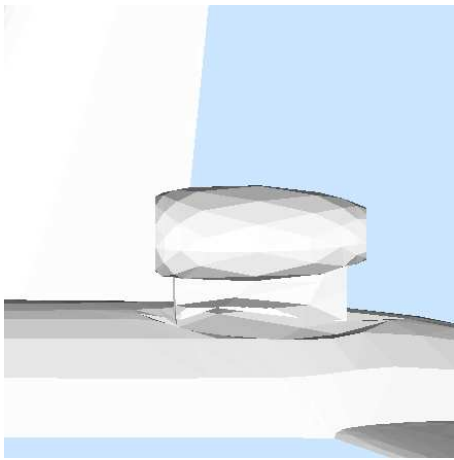
depicted the resulting shape modifications, and in Figure 10 the improvement in pressure regularity. However, the objective functional measuring the **global** smoothness of the pressure skin distribution was only reduced from $7.39 \cdot 10^{-4}$ to $7.37 \cdot 10^{-4}$. This has been obtained in 4 iterations and 29 minutes of CPU.

b- Uniformization of the pressure near the cabin

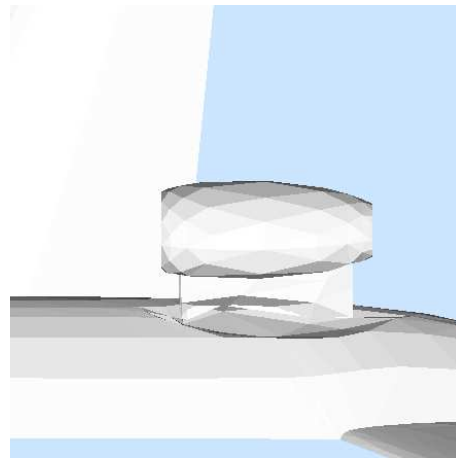
A similar process is applied in order to have a more uniform pressure on the body after the cabin. The whole section of the body is allowed to change from the cabin to near the wing (Figure 11) ; the (same) objective functional is again weakly reduced, from $7.9 \cdot 10^{-4}$ to $7.6 \cdot 10^{-4}$. This has been obtained in 4 iterations and 48 minutes of CPU, and the more uniform pressure distribution can be observed in Figure 13 ; in Figure 13, indeed, we observe that the pressure distribution is improved after the cabin ; we also observe that there is a strong influence of the geometry modification on the pressure near wing-body junction, which, within the limits of the accuracy of our simplified and coarse computation, justifies to compute with the whole geometry and to take into account the whole skin pressure in the functional instead of considering a shape



a- Initial shape of the aircraft near the engine-pylon-body junction.



b- Final shape (optimization).

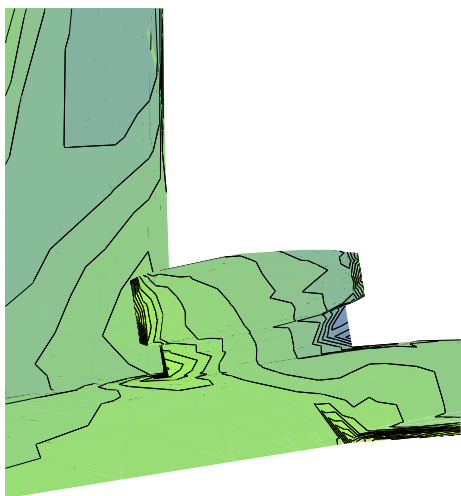


c- Final shape (One-Shot).

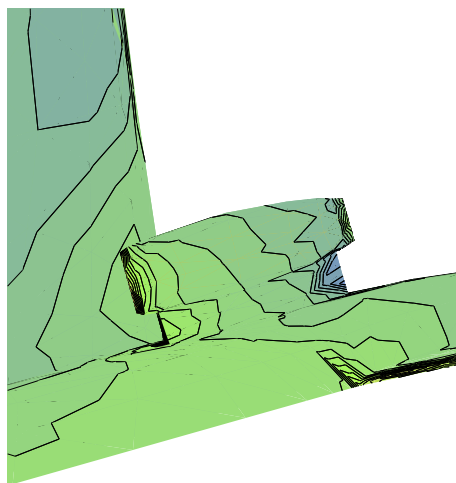
Figure 11: Optimization of the engine-pylon-body junction. For the optimization method, 4 iterations are applied ; 15 iterations are applied for the One-Shot method.

optimization process applied on a part of the flow.

In Figure 14 are depicted the initial and final shapes with and without amplification of the modification.

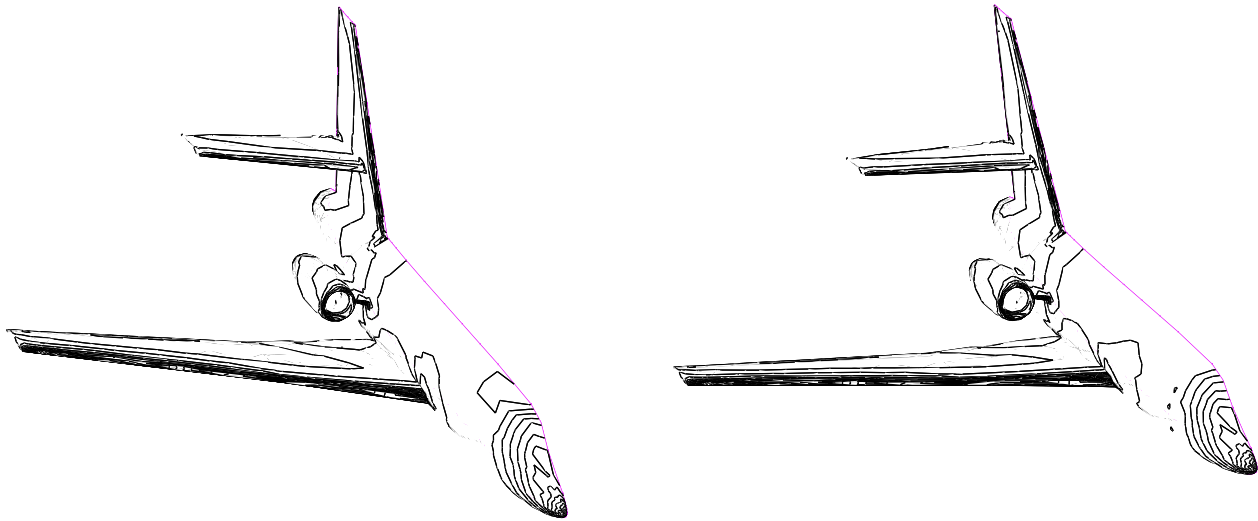


Initial pressure contours ; note the high pressures at the front part of the pylon.



Final pressure contours ; pressure levels on pylon and body are now lower.

Figure 12: Optimization of the engine-pylon-body junction ; effect of the shape optimization on the pressure contours.



a- Pressure contours for the initial shape ;
note a lower-pressure region after the cabin.

b- Pressure contours for the final shape
after 4 iterations of shape optimization.

Figure 13: Research of a more uniform pressure after the cabin : comparison of pressure contours.



a- Initial shape.



b- Final shape.



c- Amplification by a factor 4 of the deformation.

Figure 14: Research of a more uniform pressure after the cabin : initial and optimized shapes.

6 Conclusion

This work is a contribution to a new generation of shape optimizers in which the unknown is the numerical definition of the shape, involving a large number of real parameters. Although this idea is natural and old, it has often been implemented with difficulty in the literature, and the most frequent option today is to introduce a small number of parameters to vary the shape ; with this small number of parameters, and in combination with cheap analysers, optimization can rely on a sensitivity analysis obtained by divided differences.

The present choice is different with respect to :

- the **accuracy in shape** representation which is allowed by the introduction of a **multilevel method** addressing problems with many unknowns,
- most importantly, the ability of the whole system to apply to **any shape** discretized by an **unstructured tetrahedrization**.

The last property is crucial for saving engineer's time and shortening delays.

Of course, the present set of methods still have some deficiencies that are due to not well solved difficulties. We list now two of them :

- the shape parametrization works well only if the initial skin mesh is regular enough.
- there is a need for a more accurate gradient, exact for second order approximation and we intend to apply an automated differentiation for this purpose [20], [6].

For accurate optimization, much finer meshes than those presented here are mandatory, and further developments are currently started for the parallelization of the whole loop. This would also yield figures concerning the gain in efficiency due to the application of the multilevel method.

Improving further the **physical modelling** is a non trivial question. We believe that the use of the transpiration approximation is not possible in combination with the need for a stretched mesh : it may be possible to use high Reynolds $k - \varepsilon$ models with wall law and transpiration, but this remains to be experimented. Conversely, for low Reynolds formulation and stretched boundary layers, variable meshes will be required, an option allowed by automated differentiation [6].

Acknowledgements : We thank J.-M. Malé and S. Lanteri for their help at several stages in the development of the demonstration, and Dassault Aviation for yielding the Falcon mesh.

References

- [1] F. BEUX and A. DERVIEUX. A Hierarchical Approach for Shape Optimization. *Engineering Computations*, 11(1):25–48, February 1994.

- [2] C. BISCHOF, A. CARLE, G. CORLISS, and A. GRIEWANK. ADIFOR : Automatic Differentiation in a Source Translator Environment. In Paul S. Wang, editor, *International Symposium on Symbolic and Algebraic Computation*, 1992.
- [3] M.-O. BRISTEAU, R. GLOWINSKI, J. PERIAUX, P. PERRIER, and O. PIRONNEAU. On the numerical solution of nonlinear problems in fluid dynamics by least squares and finite element methods (I). least squares formulation and conjugate gradient solutions of the continuous problems. *Comput. Meths. Appl. Mech. Engrg.*, (17/18):619–657, 1979.
- [4] H. GUILLARD and N. MARCO. Some aspects of Multigrid Methods on Non-Structured meshes. In *Proceedings of the Conference of Copper Mountain on Multigrid Methods (SIAM 95)*, April 1995.
- [5] W. HACKBUSCH. *Multi-Grid Methods and Applications*, volume 4 of *Springer Series in Computational Mathematics* Springer Verlag. 1985.
- [6] M. HAFEZ, B. MOHAMMADI, and O. PIRONNEAU. Reverse Mode and Automatic Differentiation of Programs and Optimal Shape Design. *To appear*, 1996.
- [7] W. P. HUFFMAN, R. G. MELVIN, D. P. YOUNG, F. T. JOHNSON, J. E. BUSSOLLETTI, M. B. BIETERMAN, and CRAIG L. HILMES. Practical Design and Optimization in Computational Fluid Dynamics. *AIAA Paper 93-3111*, 1993.
- [8] G. KURUVILA, S. TA'ASAN, and M.D. SALAS. Airfoil Optimization by the One-Shot method. *AIAA paper*, 1994.
- [9] M.-H. LALLEMAND, H. STEVE, and A. DERVIEUX. Unstructured multigriding by volume agglomeration : current status. *Computer Fluids*, 21(3):397–433, 1992.
- [10] J.-L. LIONS. *Contrôle optimal de systèmes gouvernés par des équations aux dérivées partielles*. Dunod Gauthier-Villars, 1968. Collection Etudes Mathématiques dirigée par P. Lelong.
- [11] N. MARCO. Optimisation de formes aérodynamiques 2d et 3d par une méthode multi-niveau en maillages non-structurés, 1995. Thesis at University of Nice, France (in French).
- [12] N. MARCO and F. BEUX. Multilevel Optimization : application to shape optimum design with a One-Shot method. Research Report 2068, INRIA Sophia-Antipolis, October 1993.
- [13] N. MARCO and A. DERVIEUX. Agglomeration method applied to the Hierarchical Parametrization of a Skin Mesh in 3D Aerodynamics, 1994. Contributions to 12th month of European Project ECARP.
- [14] B. MOHAMMADI and O. PIRONNEAU. New Tools for Automatic Aerodynamic Shape Design, 1995. To appear in the book : CFD Review 95.
- [15] G.D. MORTCHELEWICZ. Résolution des équations d'Euler tridimensionnelles stationnaires en maillages non structurés. *La Recherche Aéronautique*, (6):17–25, Novembre-Décembre 1991.

-
- [16] J. MOSER. A new technique for the construction of solutions of nonlinear equations. *Proc. Nat. Acad. Sci.*, 47:1824–1831, 1961.
 - [17] F. MURAT and J. SIMON. Sur le contrôle par un domaine géométrique, 1976. Laboratoire d'Analyse Numérique, Université Paris VI.
 - [18] J. NEČAS. *Les méthodes directes en théorie des équations elliptiques*. Masson, Paris, 1967.
 - [19] J. REUTHER and A. JAMESON. Aerodynamic Shape Optimization of Wing and Wing-Body Configurations Using Control Theory. AIAA Paper 95-0123, 1995. 33rd Aerospace Sciences Meeting and Exhibit.
 - [20] N. ROSTAING-SCHMIDT and S. DALMAS. Automatic analysis and transformation of fortran programs using a typed functional language. Research Report 1518, INRIA Sophia-Antipolis, 1991.



Unité de recherche INRIA Lorraine, Technopôle de Nancy-Brabois, Campus scientifique,
615 rue du Jardin Botanique, BP 101, 54600 VILLERS LÈS NANCY
Unité de recherche INRIA Rennes, Irisa, Campus universitaire de Beaulieu, 35042 RENNES Cedex
Unité de recherche INRIA Rhône-Alpes, 655, avenue de l'Europe, 38330 MONTBONNOT ST MARTIN
Unité de recherche INRIA Rocquencourt, Domaine de Voluceau, Rocquencourt, BP 105, 78153 LE CHESNAY Cedex
Unité de recherche INRIA Sophia-Antipolis, 2004 route des Lucioles, BP 93, 06902 SOPHIA-ANTIPOLIS Cedex

Éditeur
INRIA, Domaine de Voluceau, Rocquencourt, BP 105, 78153 LE CHESNAY Cedex (France)
ISSN 0249-6399